



**HAL**  
open science

## **Biomechanics of atherosclerotic coronary plaque: site, stability and in vivo elasticity modeling.**

Jacques Ohayon, Gérard Finet, Simon Le Floc'h, Guy Cloutier, Ahmed M. Gharib, Julie Heroux, Roderic I. Pettigrew

► **To cite this version:**

Jacques Ohayon, Gérard Finet, Simon Le Floc'h, Guy Cloutier, Ahmed M. Gharib, et al.. Biomechanics of atherosclerotic coronary plaque: site, stability and in vivo elasticity modeling.. *Annals of Biomedical Engineering*, 2014, 42 (2), pp.269-279. 10.1007/s10439-013-0888-1 . hal-01017130

**HAL Id: hal-01017130**

**<https://hal.science/hal-01017130>**

Submitted on 25 Mar 2016

**HAL** is a multi-disciplinary open access archive for the deposit and dissemination of scientific research documents, whether they are published or not. The documents may come from teaching and research institutions in France or abroad, or from public or private research centers.

L'archive ouverte pluridisciplinaire **HAL**, est destinée au dépôt et à la diffusion de documents scientifiques de niveau recherche, publiés ou non, émanant des établissements d'enseignement et de recherche français ou étrangers, des laboratoires publics ou privés.



Published in final edited form as:

*Ann Biomed Eng.* 2014 February ; 42(2): 269–279. doi:10.1007/s10439-013-0888-1.

## Biomechanics of Atherosclerotic Coronary Plaque: Site, Stability and *In Vivo* Elasticity Modeling

Jacques Ohayon<sup>1,2</sup>, Gérard Finet<sup>3</sup>, Simon Le Floc'h<sup>4</sup>, Guy Cloutier<sup>5</sup>, Ahmed M. Gharib<sup>6</sup>, Julie Heroux<sup>6</sup>, and Roderic I. Pettigrew<sup>6,7</sup>

<sup>1</sup>Laboratory TIMC-IMAG/DyCTiM, UJF, CNRS UMR 5525, In3S, Grenoble, France

<sup>2</sup>Polytech Annecy-Chambéry, University of Savoie, Le Bourget du Lac, France

<sup>3</sup>Department of Hemodynamics and Interventional Cardiology, Hospices Civils de Lyon and Claude Bernard University Lyon 1, INSERM Unit 886, Lyon, France

<sup>4</sup>Laboratory LMGC, CNRS UMR 5508, University of Montpellier II, Montpellier, France

<sup>5</sup>Laboratory of Biorheology and Medical Ultrasonics, University of Montreal Hospital Research Center (CRCHUM), Montreal, QC, Canada

<sup>6</sup>Laboratory of Integrative Cardiovascular Imaging Science, National Institute of Diabetes Digestive and Kidney Diseases, National Institutes of Health, Bethesda, MD, USA

<sup>7</sup>National Institute of Biomedical Imaging and Bioengineering, National Institutes of Health, Building 31, Room 1C14, Bethesda, MD 20892-2281, USA

### Abstract

Coronary atheroma develop in local sites that are widely variable among patients and are considerably variable in their vulnerability for rupture. This article summarizes studies conducted by our collaborative laboratories on predictive biomechanical modeling of coronary plaques. It aims to give insights into the role of biomechanics in the development and localization of atherosclerosis, the morphologic features that determine vulnerable plaque stability, and emerging *in vivo* imaging techniques that may detect and characterize vulnerable plaque. Composite biomechanical and hemodynamic factors that influence the actual site of development of plaques have been studied. Plaque vulnerability, *in vivo*, is more challenging to assess. Important steps have been made in defining the biomechanical factors that are predictive of plaque rupture and the likelihood of this occurring if characteristic features are known. A critical key in defining plaque vulnerability is the accurate quantification of both the morphology and the mechanical properties of the diseased arteries. Recently, an early IVUS based palpography technique developed to assess local strain, elasticity and mechanical instabilities has been successfully revisited and improved to account for complex plaque geometries. This is based on an initial best estimation of the plaque components' contours, allowing subsequent iteration for elastic modulus assessment as a basis for plaque stability determination. The improved method has also been preliminarily evaluated in

patients with successful histologic correlation. Further clinical evaluation and refinement are on the horizon.

### Keywords

Atherosclerotic plaque; Coronary artery disease; Arterial remodeling; Biomechanics wall stress and elastic modulus; Modeling; Young's modulus

---

## INTRODUCTION

Atherosclerosis is a chronic inflammatory disease with systemic manifestations.<sup>27,53</sup> Although the coronary and peripheral systems in their entirety are exposed to the same atherogenic cells and molecules in the plasma, atherosclerotic lesions form at specific regions of the arterial tree. Such lesions appear in the vicinity of branch points, the outer wall of bifurcations and the inner wall of curves.<sup>14,34,80</sup> Pathologic studies,<sup>42</sup> have shown that healed plaque ruptures are predominantly in the proximal portions of the left anterior descending (LAD), right coronary (RCA), left circumflex (LCx) and left main (LM) arteries. Investigations over the last decade have elucidated both fluid mechanical<sup>32,43,58</sup> and most recently structural biomechanical<sup>20,30,62</sup> factors that mediated the site of plaque formation.

The coronary arterial wall is constantly subjected to both flow-induced wall shear stress (WSS) and arterial strain by blood pressure, myocardial contraction and local biological environment. Low or oscillatory WSS is one well described mechanical stimulus that promotes the inflammatory process by inducing an oxidative response in endothelial vascular cells.<sup>49</sup> Several biological studies performed on cultured endothelial cells have reported that, above an endothelial cyclic stretch threshold of 10%, endothelial cell sensitivity to shear stress increases, lowering the threshold beyond which WSS induces structural responses.<sup>48,50,51</sup> Thus, vascular remodeling is a response to alterations in WSS and other mechanical factors.

The morphologic characteristics of vulnerable coronary plaque have now been well defined in numerous pathological studies.<sup>25,59,77</sup> Typically, such plaques have a large extracellular necrotic core and a thin fibrous cap (less than 65  $\mu\text{m}$ ) infiltrated by macrophages. Clinical and biomechanical studies have identified plaque composition and morphology as key predictors of vulnerability and likelihood of rupture.<sup>54,70</sup> Such vulnerable plaques can be directly or indirectly visualized by various techniques, including intravascular ultrasound (IVUS),<sup>6,68</sup> optical coherence tomography,<sup>37,44</sup> computed tomography<sup>23</sup> and magnetic resonance imaging.<sup>5</sup> However, identifying lesions vulnerable to rupture and characterizing them as such remains a major issue for the prevention of acute thrombotic events.<sup>67</sup>

Although our knowledge of vulnerable plaque features has certainly advanced, predicting vulnerable coronary plaque rupture is still imprecise. Indeed, the thickness of the fibrous cap ( $\text{Cap}_{\text{thick}}$ ) is an important factor, but this alone is not a sufficient predictor of plaque stability.<sup>78</sup> For example, Virmani *et al.*,<sup>78</sup> in a series of 200 cases of sudden death, found that while 60% of acute thrombi resulted from rupture of a thin fibrous atheromatous cap, 70% of the same patients presented similar vulnerable appearing lesions without rupture.

Thus thin-cap fibroatheroma do not all have the same likelihood of rupture; other morphological characteristics must be involved, and this group emphasized the need for biomechanical studies to help define such relationships.<sup>78</sup>

The challenge to predict plaque rupture based on morphological characteristics of vulnerable plaques is largely due to the complexity of the biological and biomechanical interactions. While cap thickness is often taken into consideration, geometric features of the necrotic core and positive remodeling had been largely unexplored as clinical morphological indices of plaque stability or instability until described by Ohayon *et al.*<sup>60</sup> The data in the literature shows a wide dispersion in the necrotic core areas, even as a percent of the wall area, that is associated with plaque rupture.<sup>26,29,42</sup> Moreover, this dispersion has not been reduced by the discordant results of the few computational studies analyzing the influence of core area on coronary plaque stability.<sup>36,54,71</sup> Although Varnava *et al.*<sup>75</sup> highlighted a direct correlation between core area and arterial remodeling index—an indicator of plaque growth—the above structural analyses did not take into consideration the positive arterial remodeling process (or expansive remodeling) described by Glagov *et al.*<sup>31</sup> Thus, it was unclear how both the plaque-growth process and necrotic core size affect thin-cap fibroatheroma peak stress (which is a predictor of rupture).

Nonetheless, the challenge for imaging based methods is that prediction of the coronary plaque rupture requires not only an accurate quantification of fibrous cap thickness<sup>78</sup> and necrotic core morphology<sup>63</sup> but also a precise knowledge of the mechanical properties of the arterial wall and plaque components.<sup>13,24</sup> Indeed, such knowledge can allow a precise evaluation of the thin-cap fibroatheroma peak stress amplitude which, in general, appears to be a good biomechanical predictor of plaque rupture.<sup>13,24,63</sup> This may be altered when local microcalcifications are present with a sufficient size—separation ratio as defined by Weinbaum's group (in this issue).<sup>55,76</sup> Fortunately, this apparently occurs in only a small percentage of plaques.<sup>39</sup>

For predictive modeling studies, analysis of plaque mechanical properties is difficult due to its heterogeneity. More precisely, establishing a modulogram of a plaque, i.e., an elasticity map, constitutes a prerequisite for a reliable computation of intraplaque stresses. Computation of such modulograms is a challenge that has been tackled by a rather large diversity of approaches.<sup>21</sup> Based on the estimation of the strain field inside the atheroma plaque obtained from various ultrasound-based techniques<sup>17,56,79</sup> and OCT,<sup>9,69,74</sup> several studies have been performed to estimate vascular elasticity maps.<sup>3,10,38,79</sup> Either direct approaches<sup>38</sup> or iterative procedures<sup>3,10,79</sup> were proposed. The iterative approaches used a central core optimization algorithm to minimize the error between computed and measured strains or displacement fields. In this context, improvement of plaque elasticity reconstruction depends on the performance of the optimization procedure. Thus, several groups<sup>12,40</sup> have developed robust optimization algorithms for extracting elastic moduli of plaque components, assuming a known plaque morphology. Nonetheless, it seems that the main issue for improving such methods relies on the preconditioning of the algorithm based on the best estimation of the plaque components' contours.

Still, few studies have been conducted in this direction.<sup>4,10</sup> Baldewsing *et al.*<sup>2</sup> developed and successfully employed an elegant parametric finite element model (PFEM) to assess the morphology of a plaque composed of an unique necrotic core. This approach has been roughly extended by the same group to the case of multiple necrotic cores: each core was considered separately and the solution was obtained by considering the superposition of non-correlated inverse problems.<sup>4</sup> Despite its robustness, this PFEM has some limitations. Indeed, this method would not be efficient enough to extract the real morphology of plaque exhibiting several neighboring necrotic cores and/or calcium inclusions, thus preventing a good diagnosis of plaque vulnerability. An early iterative approach to this problem with initial clinical evaluation is reviewed. This is based on the integration of an automatic segmentation process over the plaque and the strain ultrasound elastographic measurements. To demonstrate the robustness of their technique relative to the original one, they studied six patients undergoing atherectomy, which allowed pathologic evaluation. Should this prove successful in thorough clinical evaluation, it could become a practical tool to detect and characterize vulnerable plaques during endovascular exploration performed in a cath lab.

This article is divided into three distinct parts, all of them describing several studies conducted by our joint laboratories on biomechanics and imaging of coronary atherosclerotic plaques:

First, we present an *in vivo* study, which investigated the contribution of myocardial contraction to the initiation of atherosclerotic lesions in coronary bifurcations. In addition to mechanical forces induced by pulsatile blood flow, coronary arteries undergo severe strain during the cardiac cycle, as they are embedded into the external layer of the epicardium.<sup>72</sup> While the effects of vessel compliance,<sup>35</sup> curvature,<sup>81</sup> blood flow<sup>66</sup> and cardiac motion on coronary WSS have been widely studied,<sup>83</sup> the effects of myocardial contraction on arterial strain distributions were previously unexplored. Surprisingly, no biomechanical study had, until recently, quantified the arterial strain distributions resulting from blood pressure and myocardium contraction acting together. Their co-influences are summarized in this review.

Second, we summarize a clinical and biomechanical study, which clarified—through an extensive computational model study—the relative roles of cap thickness, necrotic core thickness and positive remodeling index on the risk of plaque rupture.

Finally, we discuss two novel IVUS imaging techniques developed by our group for the *in vivo* mechanical characterization and detection of vulnerable coronary atherosclerotic plaques. These methods are based on a priori computation of strain elastograms to derive Young's moduli of plaque components. The methods reviewed are modulography and our improved palpography imaging techniques.

## PROCESSES INFLUENCING CORONARY PLAQUE SITE

Plaque formation is now recognized as an inflammatory process triggered by high levels of serum LDL that enter the coronary wall, encounter oxygen reactive species, and become oxidized. The oxidation, in turn, stimulates the recruitment of monocytes that convert to

macrophages to phagocytize oxidized LDLs.<sup>28,53</sup> This forms a necrotic core with recruitment of smooth muscle cells from the media to seal over the fatty core.<sup>15</sup> Flow-induced WSS is now well established as being a critical determinant of the specific sites at which this intra-wall process develops,<sup>11,65</sup> explaining in part its focal nature given that the same serum courses throughout the vascular system. In addition to local fluid mechanical differences, there are also solid mechanical variances that are contributory. Like most biological materials, the vascular wall stiffens as it is stretched.<sup>33</sup> This nonlinear elastic response may well be critical for the biological function of endothelial cells and smooth muscle cells.<sup>49,50</sup> The local wall-strain stiffening phenomenon is a local process resulting from increased local coronary wall stiffness, with strain due to the nonlinear mechanical properties of the arterial wall.<sup>33</sup>

This, in addition to low WSS and cyclic stretch, has been recently shown to be a complementary factor in plaque location in coronary bifurcations.<sup>62</sup> In patients with minimal coronary disease who had undergone both computed tomography and magnetic resonance imaging, the LM coronary bifurcation geometries were reconstructed with quantification of the kinematic constraints imposed on the coronary branches by the contracting myocardium. Using these 3D reconstructions and kinematic measurements, nonlinear computational structural analysis was performed to investigate the effects of cardiac motion and blood pressure on spatial luminal arterial wall stretch ( $LW_{stretch}$ ) and stiffness ( $LW_{stiff}$ ) distributions in left main coronary bifurcations. This approach enabled correlations between  $LW_{Stretch}$ ,  $LW_{Stiff}$  and plaque sites to be investigated. Anatomic coronary geometries and cardiac motion were generated based on both computed tomography and magnetic resonance imaging examinations of eight patients with minimal coronary disease. Computational structural finite element analysis was used to calculate  $LW_{stretch}$  and  $LW_{stiff}$  distributions in left main coronary bifurcations. Our results show that all plaque sites were concomitantly subject to high  $LW_{Stretch}$  with a mean amplitude of  $34.7 \pm 1.6\%$  and high  $LW_{Stiff}$ , with a mean amplitude of  $442.4 \pm 113.0$  kPa. The  $LW_{Stiff}$  amplitude was found to be slightly greater at the plaque sites in the LM coronary (mean value,  $482.2 \pm 88.1$  kPa) as compared to those computed in the LAD and LCx coronaries ( $416.3 \pm 61.5$  kPa and  $428.7 \pm 181.8$  kPa, respectively). These findings suggest that local wall stiffness plays a role in the initiation of atherosclerotic lesions.

Figure 1 strengthens this key finding. It considers only arterial wall regions (of approximately 12 mm in length) typical for low WSS and thus, favoring plaque deposition. However, this figure shows that among these regions, those found to have plaques also have significantly higher mean luminal arterial wall stiffness.

## MORPHOLOGIC FEATURES INFLUENCING STABILITY

To understand the evolution of plaque vulnerability during lesion development, we conducted a large scale computational analysis<sup>60</sup> that simulated a wide range of morphologies, which included the compensatory atherosclerotic arterial enlargement mechanism described by Glagov *et al.*<sup>31</sup> Such an approach enabled us to investigate the effects of anatomical necrotic core features on peak cap stress ( $Cap_{stress}$ ) during plaque evolution. Coronary lesion geometries from 24 *in vivo* IVUS cases were used to test and

validate the plaque-growth model used in this extensive computational analysis. Fibrous cap thickness ( $Cap_{thick}$ ) has been considered as diagnostic of the degree of plaque instability with  $< 65$  microns as generally indicative of vulnerability. Necrotic core area ( $Core_{area}$ ) and the arterial remodeling index ( $Remod_{index} = \text{Abnormal Diameter}/\text{Normal Diameter}$ ) on the other hand, have been historically viewed as among the determinant factors of plaque vulnerability. Literature data show a wide dispersion of  $Core_{area}$  thresholds above which a plaque becomes unstable. Although histopathology shows a strong correlation between  $Core_{area}$  and  $Remod_{index}$ ,<sup>75</sup> it had been unclear how these factors interact and affect peak cap stress ( $Cap_{stress}$ )—a known predictor of rupture. Our computational study was therefore designed to investigate the effects of necrotic core size and plaque morphology on risk of plaque rupture.

In order to take full advantage of the arterial remodeling process described by Glagov *et al.*,<sup>31</sup> the atherosclerotic plaque was considered as a three-dimensional structure, but under a plane strain condition. This assumption is reasonable insofar as (i) plaque length is large with regard to the radial dimension, and (ii) neighboring cross-sectional morphologies remain similar.<sup>16,61</sup> However, to overcome the limitations entailed by the plane strain assumption, two additional and more realistic three-dimensional plaque geometries were considered, slightly modifying the three-dimensional “plane strain” model (data not shown). In the first one, cap thickness varied while necrotic core thickness and plaque length remained constant. In the second case, cap thickness was kept constant while necrotic core thickness varied.  $Cap_{stress}$  values were then computed within the plaque cross-section where the cap thickness was the thinnest (first case) or where the necrotic core thickness was the largest (second case). We found that the variation in  $Cap_{stress}$  computed with or without the plane strain assumption did not exceed 25%. For these models, material properties were taken from the literature.<sup>82</sup> Such results agree with those obtained by Cilla *et al.*<sup>16</sup> when considering the full 3D FE model of atherosclerotic plaque.

$Cap_{stress}$  value was calculated on 5500 idealized atherosclerotic vessel models. Taking advantage of these extensive simulations, the effects of anatomical plaque features on  $Cap_{stress}$  were investigated. These comprehensive simulations are summarized in Fig. 2. This 3D graphic shows the relative and quantitative contributions to plaque instability by arterial remodeling index, necrotic core thickness and critical cap thickness, as defined by the peak cap stress reaching the rupture threshold of 300 kPa. This analysis shows: (i) at the early stages of positive remodeling, lesions with large % necrotic core thickness were more prone to rupture, which could explain the progression and growth of clinically silent plaques; and (ii) in addition to cap thickness and remodeling index, necrotic core thickness—rather than area—was critical in determining plaque stability. This study demonstrates that plaque instability is not a consequence of fibrous cap thickness alone, but rather is dependent on a complex but generally understandable combination of cap thickness, necrotic core thickness and the arterial remodeling index.

This relationship may offer some insight into the observation that more than half of myocardial infarctions originate in vessels with relatively small stenosis (i.e.,  $Stenos_{deg} < 50\%$ ).<sup>28,41,75</sup> Lee’s group,<sup>54</sup> in their structural analysis, explored the influence of  $Stenos_{deg}$ . However, in their models, increasing  $Stenos_{deg}$  induced an increase in  $Cap_{thick}$ .

which in turn reduced the stress in the fibrous cap. Moreover, their analyses were restricted to high values of arterial stenosis (i.e.,  $70\% < \text{Stenos}_{\text{deg}} < 99\%$ ), which correspond to arterial remodeling indexes above 1.6 in Fig. 2. In this range of stenosis, results have shown a limited influence of the necrotic core thickness. Thus, no conclusion about the plaque stability at early stages of the arterial remodeling process could be inferred from their study. We therefore investigated the effect of  $\text{Stenos}_{\text{deg}}$  alone on plaque stability by considering the arterial remodeling process which occurs in response to plaque growth. Interestingly, among all plaque topologies those with a large relative  $\text{Core}_{\text{thick}}$  and small  $\text{Stenos}_{\text{deg}}$  were found to be more likely to rupture. This finding is consistent with Varnava *et al.*'s findings<sup>75</sup> that plaque rupture often occurs at sites with relatively small luminal stenosis. In addition, it shows that once the % necrotic core reaches ~50%, positive arterial remodeling serves to reduce the cap stress so that thinner caps can be reached before rupture occurs. As such, positive arterial remodeling can be viewed as a protective mechanism that not only preserves vessel lumen diameter, but also retards plaque rupture, albeit with limits.

Since this study and analysis was performed, the role of closely spaced microcalcifications—which appear to occur in 2% of examined post mortem samples—has been studied.<sup>39</sup> Though difficult to detect clinically, this is another consideration as described in this issue by Weinbaum's group. Interestingly, the results of Fig. 2 could be combined with the effect of  $\mu\text{Calcs}$  highlighted by Kelly-Arnold *et al.*,<sup>39</sup> which have shown that  $\mu\text{Calcs}$  between 5 and 15  $\mu\text{m}$  would increase the  $\text{Cap}_{\text{stress}}$  by at least a factor of two.

## MODELING PLAQUE STABILITY

Modeling individual plaque stability requires knowledge of the elasticity or Young's modulus of the plaque components, as well as the geometries thereof.<sup>24</sup> Quantifying intraplaque stress distribution to predict plaque rupture, has been a challenge. To overcome this hurdle, the rate of deformation (strain) of a tissue can be calculated and directly related to the intraplaque stress and its mechanical properties. Ophir and colleagues<sup>8,64</sup> pioneered developing imaging techniques based on the strain field. Based on their work, several elegant IVUS methods were developed to highlight the spatial strain distribution (i.e., strain-elastogram) over the entire vessel wall<sup>57</sup> or over a restricted thick endoluminal region.<sup>18,22</sup> Such IVUS techniques, based on the optical flow<sup>57</sup> or time-delay correlation estimation,<sup>17</sup> allowed the calculations of intraplaque strain images during the cardiac cycle. However, these methods did not overcome a main limitation related to the complex geometries of atherosclerotic plaques, which alter the intraplaque strain fields and inhibit direct translation into plaque mechanical properties.

Therefore we designed an initial theoretical study to determine the modulogram of complex atherosclerotic plaques by developing an original preconditioning step for the optimization process, and a new approach combining a dynamic watershed segmentation method with the optimization procedure to extract the morphology and Young's modulus of each plaque component. This combined approach, based on the continuum mechanics theory prescribing the strain field, has been successfully applied to coronary lesions of a small number of patients imaged *in vivo* with IVUS and with concurrent atherectomies. This method was investigated to assess important factors for the prediction of plaque vulnerability.



This new approach, called iMOD, reconstructs elasticity maps (or modulograms) of atheroma plaques from the estimation of strain fields.<sup>47</sup> To test the performance and accuracy of this approach, an *in vitro* experimental study was conducted on PVA-C arterial phantoms. The benefit of coupling the iMOD procedure with the acquisition of IVUS measurements for detection of vulnerable plaque was also investigated.<sup>46</sup> The results showed that the combined iMOD-IVUS strategy : (i) successfully detected and quantified soft inclusion contours with high positive predictive values and sensitivities of  $89.7 \pm 3.9$  and  $81.5 \pm 8.8\%$ , respectively, (ii) reasonably estimated cap thicknesses larger than  $\sim 300$   $\mu\text{m}$ , but underestimated thinner caps, and (iii) satisfactorily quantified the Young's modulus of hard medium (mean value of  $109.7 \pm 23.7$  instead of  $145.4 \pm 31.8$  kPa), but overestimated the stiffness of soft inclusions (mean Young's moduli of  $31.4 \pm 9.7$  instead of  $17.6 \pm 3.4$  kPa).

*In vivo* IVUS modulography, however, remains a major challenge as the motion of the heart prevents accurate strain field estimation. Thus a modified technique has been developed to extract accurate strain fields and modulograms from recorded IVUS sequences. A set of four criteria was identified based on the temporal assessment of overlapping tissue with a RF-correlation coefficient between two successive frames, the performance of the elasticity reconstruction method to recover the measured radial strain, and the reproducibility of the computed modulograms over the cardiac cycle. As below, this four-criterion selection procedure (4-CSP) was successfully tested on IVUS sequences obtained in twelve patients referred for a directional coronary atherectomy intervention.<sup>45</sup> As such, this study demonstrates the potential of the IVUS modulography technique based on the proposed 4-CSP to detect vulnerable plaques *in vivo*.

From the IVUS echogram and strain images, Céspedes *et al.*<sup>7</sup> proposed an elasticity-palpography technique (E-PT) to estimate the apparent stress-strain modulus (S-SM) palpogram of the thick endoluminal layer of the arterial wall. However, this approach suffers from major limitations because it was developed for homogeneous, circular and concentric VPs. The approach of Deleaval *et al.*<sup>19</sup> was therefore designed to improve the E-PT by considering all anatomical shapes of vulnerable plaques, including eccentric lesions.

The details of both the improved S-SM palpography technique and the 4-CSP approach to solving the inverse problem of deciphering moduli from serial IVUS images are described in Deleaval *et al.*<sup>19</sup> and Le Floch *et al.*,<sup>45</sup> respectively. As regards the 4-CSP method, for each patient's atherosclerotic lesion, approximately 30 displacement maps were reconstructed based on the IVUS sequence recorded during one second. Then four criteria were used to extract accurate displacement, strain and elasticity maps. The first criterion estimates the quality of the measured displacement field (displacement quality index  $Q_{\text{displa}}$ ); the second criterion estimates the accuracy of the spatial distribution of the RF-correlation coefficient between two successive frames (tracking quality index  $Q_{\text{track}}$ ); the third criterion estimates the propensity of the Young's modulus reconstruction method to recover the measured radial strain (strain quality index  $Q_{\text{strain}}$ ); finally, the last criterion estimates the reproducibility of resulting modulograms over the cardiac cycle (reproducibility quality index  $Q_{\text{reprod}}$ ). The performance of this approach is illustrated in Fig. 3, based on *in vivo* imaging and histologic evaluations (Fig. 4). This 4-CSP was successfully tested on IVUS

sequences obtained in twelve patients referred for a directional coronary atherectomy intervention. This initial study demonstrates the potential of the IVUS modulography technique based on the proposed 4-CSP to detect vulnerable plaques *in vivo*. Although these new *in vivo* imaging techniques may help detect and diagnose the degree of plaque stability, such models need to be extended to include the nonlinear and anisotropic behaviors of the artery and plaque components. A subsequent palpography study proposed by Deleaval *et al.*<sup>19</sup>—which allows a fast wall stiffness quantification based on the arterial strain and blood pressure measurements (Fig. 5)—shows further improvements which account for the specific shape of the plaque with complex geometries, noise and blood pressure. Overall, these studies demonstrate the potential for second generation IVUS modulography techniques based on these new criteria to detect vulnerable plaques *in vivo*. In diagnostic cardiovascular medicine, this is a horizon in which bioengineering is playing an essential role.

## POTENTIAL CLINICAL IMPLICATIONS

Acute coronary syndromes are caused by an occlusion of the lumen by thrombi formed secondary to a ruptured atherosclerotic plaque or fissuring in the atherosclerotic wall.<sup>28</sup> There are several major mechanisms causing plaque disruption, including plaque erosion,<sup>28,77</sup> tissue degradation due to macrophage infiltration<sup>28,41,59</sup> and components of biological processes that comprise the cellular inflammatory reaction.<sup>1,28,73</sup> *In vivo* imaging techniques could help provide a better understanding of the evolution of plaque composition and morphology during the arterial remodeling and growth process. The instability of a vulnerable plaque is mainly caused by the large mechanical stress that develops in the thinnest part of the fibrous cap. It has been shown that this peak cap stress amplitude—a biomechanical predictor of plaque rupture—varies exponentially not only with cap thickness, but also with Young's modulus of the necrotic core.<sup>24</sup> Several animal and clinical studies conducted to analyze the structural variation in the fibrous cap and necrotic core demonstrated that treatment with statins enhances plaque stability.<sup>52</sup> Our cap stress analysis shows how very slight structural changes can tilt a vulnerable plaque from stability to instability or *vice versa* and thus how statins might indeed make a clinically significant difference in plaque stability. As this analysis points out, such small changes in Young's Modulus may either 'precipitate' rupture or, conversely, 'stabilize' a vulnerable plaque. The *in vivo* use of the proposed imaging method may allow studying the evolution of the mechanical stability of atherosclerotic plaques. Additionally, the proposed method may allow elucidating the process by which during the first few weeks to months of statin therapy, vulnerable plaques tend to become more stable. This may likely be attributed to changes in mechanical properties of plaque constituents, namely the hardening of the necrotic core, as suggested by our previous finite element simulations.<sup>24</sup>

## Acknowledgments

The authors would like to thank Shadi Mamaghani, Ph.D. for her expert assistance in the review and editing of the manuscript. This research was supported in part by an appointment (J. Ohayon) to the Senior Fellow Program at the National Institutes of Health (NIH) 2006–2007. This program was administered by Oak Ridge Institute for Science and Education through an interagency agreement between the NIH and the U.S. Department of Energy. J. Ohayon, G. Cloutier and G. Finet were supported by grants from the Région Rhône-Alpes (2010–2013), the Agence Nationale de la Recherche (ANR), France (ATHEBIOMECH project # 06-BLANC-0263), and by the collaborative

health research joint program of the Natural Sciences and Engineering Research Council of Canada (NSERC #323405-06) and Canadian Institutes of Health Research (CIHR #CPG-80085). This research is now supported by a joint international program of the ANR (MELANII project # 09-BLANC-0423) and NSERC strategic grant #STPGP-381136-09.

## References

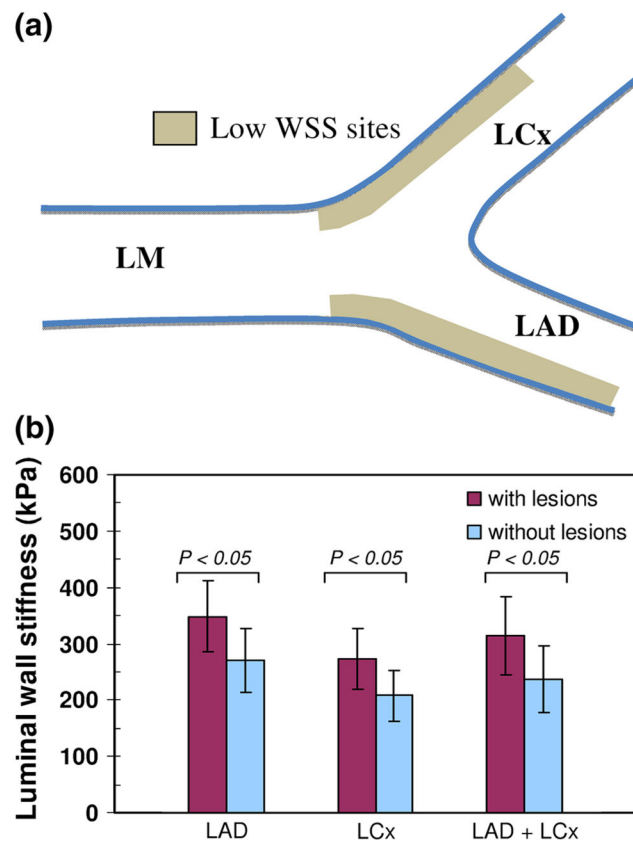
1. Arroyo LH, Lee RT. Mechanisms of plaque rupture: mechanical and biologic interactions. *Cardiovasc Res.* 1999; 41:369–375. [PubMed: 10341836]
2. Baldewsing RA, Mastik F, Schaar JA, Serruys PW, van der Steen AF. Young's modulus reconstruction of vulnerable atherosclerotic plaque components using deformable curves. *Ultrasound Med Biol.* 2006; 32:201–210. [PubMed: 16464666]
3. Baldewsing RA, Schaar JA, Mastik F, Oomens CW, van der Steen AF. Assessment of vulnerable plaque composition by matching the deformation of a parametric plaque model to measured plaque deformation. *IEEE Trans Med Imaging.* 2005; 24:514–528. [PubMed: 15822809]
4. Baldewsing RA, Schaar JA, Mastik F, van der Steen AF. Local elasticity imaging of vulnerable atherosclerotic coronary plaques. *Adv Cardiol.* 2007; 44:35–61. [PubMed: 17075198]
5. Briley-Saebo KC, Mulder WJ, Mani V, Hyafil F, Amirbekian V, Aguinaldo JG, Fisher EA, Fayad ZA. Magnetic resonance imaging of vulnerable atherosclerotic plaques: current imaging strategies and molecular imaging probes. *J Magn Reson Imaging.* 2007; 26:460–479. [PubMed: 17729343]
6. Carlier SG, Tanaka K. Studying coronary plaque regression with IVUS: a critical review of recent studies. *J Interv Cardiol.* 2006; 19:11–15. [PubMed: 16483334]
7. Cespedes EI, de Korte CL, van der Steen AF. Intraluminal ultrasonic palpation: assessment of local and cross-sectional tissue stiffness. *Ultrasound Med Biol.* 2000; 26:385–396. [PubMed: 10773368]
8. Cespedes I, Ophir J, Ponnekanti H, Maklad N. Elastography: elasticity imaging using ultrasound with application to muscle and breast in vivo. *Ultrason Imaging.* 1993; 15:73–88. [PubMed: 8346612]
9. Chan RC. OCT-based arterial elastography: robust estimation exploiting tissue biomechanics. *Opt Express.* 2004; 12:4558–4572. [PubMed: 19484007]
10. Chandran KB, Mun JH, Choi KK, Chen JS, Hamilton A, Nagaraj A, McPherson DD. A method for in vivo analysis for regional arterial wall material property alterations with atherosclerosis: preliminary results. *Med Eng Phys.* 2003; 25:289–298. [PubMed: 12649013]
11. Chatzizisis YS, Coskun AU, Jonas M, Edelman ER, Feldman CL, Stone PH. Role of endothelial shear stress in the natural history of coronary atherosclerosis and vascular remodeling: molecular, cellular, and vascular behavior. *J Am Coll Cardiol.* 2007; 49:2379–2393. [PubMed: 17599600]
12. Chau AH, Chan RC, Shishkov M, MacNeill B, Iftimia N, Tearney GJ, Kamm RD, Bouma BE, Kaazempur-Mofrad MR. Mechanical Analysis of Atherosclerotic Plaques Based on Optical Coherence Tomography. *Ann Biomed Eng.* 2004; 32:1494. [PubMed: 15636110]
13. Cheng GC, Loree HM, Kamm RD, Fishbein MC, Lee RT. Distribution of circumferential stress in ruptured and stable atherosclerotic lesions. A structural analysis with histopathological correlation. *Circulation.* 1993; 87:1179–1187. [PubMed: 8462145]
14. Cheruvu PK, Finn AV, Gardner C, Caplan J, Goldstein J, Stone GW, Virmani R, Muller JE. Frequency and distribution of thin-cap fibroatheroma and ruptured plaques in human coronary arteries: a pathologic study. *J Am Coll Cardiol.* 2007; 50:940–949. [PubMed: 17765120]
15. Choudhury RP, Fuster V, Fayad ZA. Molecular, cellular and functional imaging of atherothrombosis. *Nat Rev Drug Discov.* 2004; 3:913–925. [PubMed: 15520814]
16. Cilla M, Pena E, Martinez MA. 3D computational parametric analysis of eccentric atheroma plaque: influence of axial and circumferential residual stresses. *Biomech Model Mechanobiol.* 2012; 11:1001–1013. [PubMed: 22227796]
17. de Korte CL, Carlier SG, Mastik F, Doyley MM, van der Steen AF, Serruys PW, Bom N. Morphological and mechanical information of coronary arteries obtained with intravascular elastography; feasibility study in vivo. *Eur Heart J.* 2002; 23:405–413. [PubMed: 11846498]
18. de Korte CL, Woutman HA, van der Steen AF, Pasterkamp G, Cespedes EI. Vascular tissue characterisation with IVUS elastography. *Ultrasonics.* 2000; 38:387–390. [PubMed: 10829693]

19. Deleaval F, Bouvier A, Finet G, Cloutier G, Yazdani SK, Le Floc'h S, Clarysse P, Pettigrew RI, Ohayon J. The intravascular ultrasound elasticity-palpography technique revisited: A reliable tool for the in vivo detection of vulnerable coronary atherosclerotic plaques. *Ultrasound Med Biol.* 2013; 39(8):1469–1481. [PubMed: 23727295]
20. Delfino A, Stergiopoulos N, Moore JE, Meister JJ. Residual strain effects on the stress field in a thick wall finite element model of the human carotid bifurcation. *J Biomech.* 1997; 30:777–786. [PubMed: 9239562]
21. Doyley MM. Model-based elastography: a survey of approaches to the inverse elasticity problem. *Phys Med Biol.* 2012; 57:R35–R73. [PubMed: 22222839]
22. Doyley MM, Mastik F, de Korte CL, Carlier SG, Cespedes EI, Serruys PW, Bom N, van der Steen AF. Advancing intravascular ultrasonic palpation toward clinical applications. *Ultrasound Med Biol.* 2001; 27:1471–1480. [PubMed: 11750745]
23. Fayad ZA, Fuster V, Nikolaou K, Becker C. Computed tomography and magnetic resonance imaging for noninvasive coronary angiography and plaque imaging: current and potential future concepts. *Circulation.* 2002; 106:2026–2034. [PubMed: 12370230]
24. Finet G, Ohayon J, Rioufol G. Biomechanical interaction between cap thickness, lipid core composition and blood pressure in vulnerable coronary plaque: impact on stability or instability. *Coron Artery Dis.* 2004; 15:13–20. [PubMed: 15201616]
25. Fleg JL, Stone GW, Fayad ZA, Granada JF, Hatsukami TS, Kolodgie FD, Ohayon J, Pettigrew R, Sabatine MS, Tearney GJ, Waxman S, Domanski MJ, Srinivas PR, Narula J. Detection of high-risk atherosclerotic plaque: report of the NHLBI Working Group on current status and future directions. *JACC Cardiovasc Imaging.* 2012; 5:941–955. [PubMed: 22974808]
26. Fujii K, Kobayashi Y, Mintz GS, Takebayashi H, Dangas G, Moussa I, Mehran R, Lansky AJ, Kreps E, Collins M, Colombo A, Stone GW, Leon MB, Moses JW. Intravascular ultrasound assessment of ulcerated ruptured plaques: a comparison of culprit and nonculprit lesions of patients with acute coronary syndromes and lesions in patients without acute coronary syndromes. *Circulation.* 2003; 108:2473–2478. [PubMed: 14610010]
27. Fuster V, Moreno PR. Atherothrombosis as a systemic, often silent, disease. *Nat Clin Pract Cardiovasc Med.* 2005; 2(9):431. [PubMed: 16265564]
28. Fuster V, Moreno PR, Fayad ZA, Corti R, Badimon JJ. Atherothrombosis and high-risk plaque: part I: evolving concepts. *J Am Coll Cardiol.* 2005; 46:937–954. [PubMed: 16168274]
29. Gertz SD, Roberts WC. Hemodynamic shear force in rupture of coronary arterial atherosclerotic plaques. *Am J Cardiol.* 1990; 66:1368–1372. [PubMed: 2244569]
30. Gijssen FJ, Wentzel JJ, Thury A, Mastik F, Schaar JA, Schuurbers JC, Slager CJ, van der Giessen WJ, de Feyter PJ, van der Steen AF, Serruys PW. Strain distribution over plaques in human coronary arteries relates to shear stress. *Am J Physiol Heart Circ Physiol.* 2008; 295:H1608–H1614. [PubMed: 18621851]
31. Glagov S, Weisenberg E, Zarins CK, Stankunavicius R, Kolettis GJ. Compensatory enlargement of human atherosclerotic coronary arteries. *N Engl J Med.* 1987; 316:1371–1375. [PubMed: 3574413]
32. He X, Ku DN. Pulsatile flow in the human left coronary artery bifurcation: average conditions. *J Biomech Eng.* 1996; 118:74–82. [PubMed: 8833077]
33. Holzapfel GA, Sommer G, Gasser CT, Regitnig P. Determination of layer-specific mechanical properties of human coronary arteries with nonatherosclerotic intimal thickening and related constitutive modeling. *Am J Physiol Heart Circ Physiol.* 2005; 289:H2048–H2058. [PubMed: 16006541]
34. Hong MK, Mintz GS, Lee CW, Lee BK, Yang TH, Kim YH, Song JM, Han KH, Kang DH, Cheong SS, Song JK, Kim JJ, Park SW, Park SJ. The site of plaque rupture in native coronary arteries: a three-vessel intravascular ultrasound analysis. *J Am Coll Cardiol.* 2005; 46:261–265. [PubMed: 16022952]
35. Huo Y, Choy JS, Svendsen M, Sinha AK, Kassab GS. Effects of vessel compliance on flow pattern in porcine epicardial right coronary arterial tree. *J Biomech.* 2009; 42:594–602. [PubMed: 19195659]

36. Imoto K, Hiro T, Fujii T, Murashige A, Fukumoto Y, Hashimoto G, Okamura T, Yamada J, Mori K, Matsuzaki M. Longitudinal structural determinants of atherosclerotic plaque vulnerability: a computational analysis of stress distribution using vessel models and three-dimensional intravascular ultrasound imaging. *J Am Coll Cardiol*. 2005; 46:1507–1515. [PubMed: 16226176]
37. Jang IK, Bouma BE, Kang DH, Park SJ, Park SW, Seung KB, Choi KB, Shishkov M, Schlenkorf K, Pomerantsev E, Houser SL, Aretz HT, Tearney GJ. Visualization of coronary atherosclerotic plaques in patients using optical coherence tomography: comparison with intravascular ultrasound. *J Am Coll Cardiol*. 2002; 39:604–609. [PubMed: 11849858]
38. Kanai H, Hasegawa H, Ichiki M, Tezuka F, Koiwa Y. Elasticity imaging of atheroma with transcutaneous ultrasound: preliminary study. *Circulation*. 2003; 107:3018–3021. [PubMed: 12810617]
39. Kelly-Arnold A, Maldonado N, Laudier D, Aikawa E, Cardoso L, Weinbaum S. Revised microcalcification hypothesis for fibrous cap rupture in human coronary arteries. *Proc Natl Acad Sci USA*. 2013; 110:10741–10746. [PubMed: 23733926]
40. Khalil AS, Bouma BE, Kaazempur Mofrad MR. A combined FEM/genetic algorithm for vascular soft tissue elasticity estimation. *Cardiovasc Eng*. 2006; 6:93–102. [PubMed: 16967325]
41. Koenig W. Inflammation and coronary heart disease: an overview. *Cardiol Rev*. 2001; 9:31–35. [PubMed: 11174913]
42. Kolodgie FD, Burke AP, Farb A, Gold HK, Yuan J, Narula J, Finn AV, Virmani R. The thin-cap fibroatheroma: a type of vulnerable plaque: the major precursor lesion to acute coronary syndromes. *Curr Opin Cardiol*. 2001; 16:285–292. [PubMed: 11584167]
43. Ku DN, Giddens DP, Zarins CK, Glagov S. Pulsatile flow and atherosclerosis in the human carotid bifurcation. Positive correlation between plaque location and low oscillating shear stress. *Arteriosclerosis*. 1985; 5:293–302. [PubMed: 3994585]
44. Kubo T, Imanishi T, Takarada S, Kuroi A, Ueno S, Yamano T, Tanimoto T, Matsuo Y, Masho T, Kitabata H, Tsuda K, Tomobuchi Y, Akasaka T. Assessment of culprit lesion morphology in acute myocardial infarction: ability of optical coherence tomography compared with intravascular ultrasound and coronary angiography. *J Am Coll Cardiol*. 2007; 50:933–939. [PubMed: 17765119]
45. Le Floc'h S, Cloutier G, Saijo Y, Finet G, Yazdani SK, Deleaval F, Rioufol G, Pettigrew RI, Ohayon J. A four-criterion selection procedure for atherosclerotic plaque elasticity reconstruction based on in vivo coronary intravascular ultrasound radial strain sequences. *Ultrasound Med Biol*. 2012; 38:2084–2097. [PubMed: 23196202]
46. Le Floc'h S, Cloutier G, Finet G, Tracqui P, Pettigrew RI, Ohayon J. On the potential of a new IVUS elasticity modulus imaging approach for detecting vulnerable atherosclerotic coronary plaques: in vitro vessel phantom study. *Phys Med Biol*. 2010; 55:5701–5721. [PubMed: 20826899]
47. Le Floc'h S, Ohayon J, Tracqui P, Finet G, Gharib AM, Maurice RL, Cloutier G, Pettigrew RI. Vulnerable atherosclerotic plaque elasticity reconstruction based on a segmentation-driven optimization procedure using strain measurements: theoretical framework. *IEEE Trans Med Imaging*. 2009; 28:1126–1137. [PubMed: 19164080]
48. Lehoux S. Redox signalling in vascular responses to shear and stretch. *Cardiovasc Res*. 2006; 71:269–279. [PubMed: 16780820]
49. Lehoux S, Castier Y, Tedgui A. Molecular mechanisms of the vascular responses to haemodynamic forces. *J Intern Med*. 2006; 259:381–392. [PubMed: 16594906]
50. Lehoux S, Esposito B, Merval R, Loufrani L, Tedgui A. Pulsatile stretch-induced extracellular signal-regulated kinase 1/2 activation in organ culture of rabbit aorta involves reactive oxygen species. *Arterioscler Thromb Vasc Biol*. 2000; 20:2366–2372. [PubMed: 11073839]
51. Lehoux S, Tedgui A. Signal transduction of mechanical stresses in the vascular wall. *Hypertension*. 1998; 32:338–345. [PubMed: 9719064]
52. Libby P, Ridker PM, Maseri A. Inflamm Atheroscler Circ. 2002; 105:1135–1143.
53. Libby P, Theroux P. Pathophysiology of coronary artery disease. *Circulation*. 2005; 111:3481–3488. [PubMed: 15983262]

54. Loree HM, Kamm RD, Stringfellow RG, Lee RT. Effects of fibrous cap thickness on peak circumferential stress in model atherosclerotic vessels. *Circ Res.* 1992; 71:850–858. [PubMed: 1516158]
55. Maldonado N, Kelly-Arnold A, Cardoso L, Weinbaum S. The explosive growth of small voids in vulnerable cap rupture; cavitation and interfacial debonding. *J Biomech.* 2013; 46:396–401. [PubMed: 23218838]
56. Maurice RL, Fromageau J, Brusseau E, Finet G, Rioufol G, Cloutier G. On the potential of the lagrangian estimator for endovascular ultrasound elastography: in vivo human coronary artery study. *Ultrasound Med Biol.* 2007; 33:1199–1205. [PubMed: 17466446]
57. Maurice RL, Ohayon J, Finet G, Cloutier G. Adapting the Lagrangian speckle model estimator for endovascular elastography: theory and validation with simulated radio-frequency data. *J Acoust Soc Am.* 2004; 116:1276–1286. [PubMed: 15376693]
58. Moore JE, Ku DN, Zarins CK, Glagov S. Pulsatile flow visualization in the abdominal aorta under differing physiologic conditions: implications for increased susceptibility to atherosclerosis. *J Biomech Eng.* 1992; 114:391–397. [PubMed: 1295493]
59. Naghavi M, Libby P, Falk E, Casscells SW, Litovsky S, Rumberger J, Badimon JJ, Stefanadis C, Moreno P, Pasterkamp G, Fayad Z, Stone PH, Waxman S, Raggi P, Madjid M, Zarrabi A, Burke A, Yuan C, Fitzgerald PJ, Siscovick DS, de Korte CL, Aikawa M, Airaksinen KE, Assmann G, Becker CR, Chesebro JH, Farb A, Galis ZS, Jackson C, Jang IK, Koenig W, Lodder RA, March K, Demirovic J, Navab M, Puri SG, Reekter MD, Bahr R, Grundy SM, Mehran R, Colombo A, Boerwinkle E, Ballantyne C, Insull W Jr, Schwartz RS, Vogel R, Serruys PW, Hansson GK, Faxon DP, Kaul S, Drexler H, Greenland P, Muller JE, Virmani R, Ridker PM, Zipes DP, Shah PK, Willerson JT. From vulnerable plaque to vulnerable patient: a call for new definitions and risk assessment strategies: Part II. *Circulation.* 2003; 108:1772–1778. [PubMed: 14557340]
60. Ohayon J, Finet G, Gharib AM, Herzka DA, Tracqui P, Heroux J, Rioufol G, Kotys MS, Elagha A, Pettigrew RI. Necrotic core thickness and positive arterial remodeling index: emergent biomechanical factors for evaluating the risk of plaque rupture. *Am J Physiol Heart Circ Physiol.* 2008; 295:H717–H727. [PubMed: 18586893]
61. Ohayon, J.; Finet, G.; Treyve, F.; Rioufol, G.; Dubreuil, O. A three-dimensional finite element analysis of stress distribution in a coronary atherosclerotic plaque: in vivo prediction of plaque rupture location. Kerala, India: Research Singpost; 2005. p. 225-241.
62. Ohayon J, Gharib AM, Garcia A, Heroux J, Yazdani SK, Malve M, Tracqui P, Martinez MA, Doblare M, Finet G, Pettigrew RI. Is arterial wall-strain stiffening an additional process responsible for atherosclerosis in coronary bifurcations?: an in vivo study based on dynamic CT and MRI. *Am J Physiol Heart Circ Physiol.* 2011; 301:H1097–H1106. [PubMed: 21685261]
63. Ohayon J, Teppaz P, Finet G, Rioufol G. In-vivo prediction of human coronary plaque rupture location using intravascular ultrasound and the finite element method. *Coron Artery Dis.* 2001; 12:655–663. [PubMed: 11811331]
64. Ophir J, Cespedes I, Ponnekanti H, Yazdi Y, Li X. Elastography: a quantitative method for imaging the elasticity of biological tissues. *Ultrason Imaging.* 1991; 13:111–134. [PubMed: 1858217]
65. Papafaklis MI, Koskinas KC, Chatzizisis YS, Stone PH, Feldman CL. In-vivo assessment of the natural history of coronary atherosclerosis: vascular remodeling and endothelial shear stress determine the complexity of atherosclerotic disease progression. *Curr Opin Cardiol.* 2010; 25:627–638. [PubMed: 20838338]
66. Perktold K, Hofer M, Rappitsch G, Loew M, Kuban BD, Friedman MH. Validated computation of physiologic flow in a realistic coronary artery branch. *J Biomech.* 1998; 31:217–228. [PubMed: 9645536]
67. Rabbani R, Topol EJ. Strategies to achieve coronary arterial plaque stabilization. *Cardiovasc Res.* 1999; 41:402–417. [PubMed: 10341840]
68. Rioufol G, Finet G, Ginon I, Andre-Fouet X, Rossi R, Vialle E, Desjoyaux E, Convert G, Huret JF, Tabib A. Multiple atherosclerotic plaque rupture in acute coronary syndrome: a three-vessel intravascular ultrasound study. *Circulation.* 2002; 106:804–808. [PubMed: 12176951]

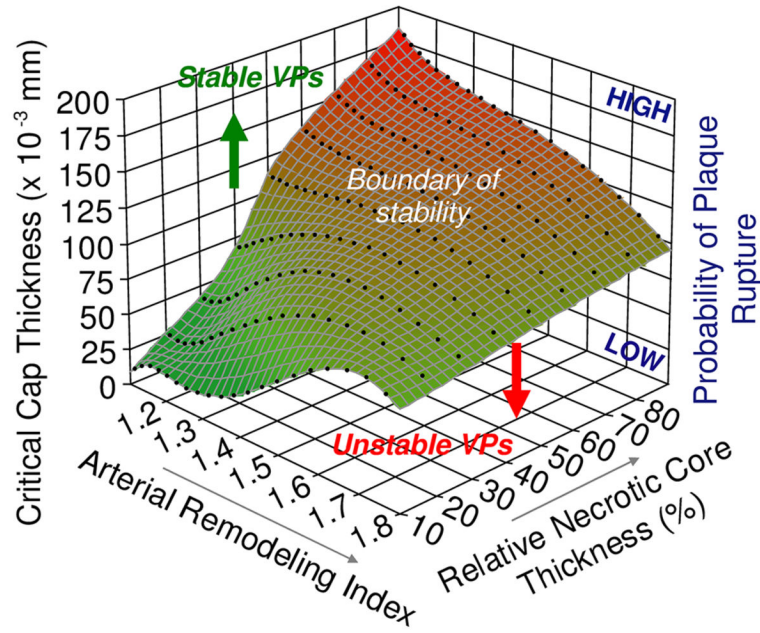
69. Rogowska J, Patel NA, Fujimoto JG, Brezinski ME. Optical coherence tomographic elastography technique for measuring deformation and strain of atherosclerotic tissues. *Heart*. 2004; 90:556–562. [PubMed: 15084558]
70. Shah PK. Plaque size, vessel size and plaque vulnerability: bigger may not be better. *J Am Coll Cardiol*. 1998; 32:663–664. [PubMed: 9741508]
71. Tang D, Yang C, Kobayashi S, Ku DN. Effect of a lipid pool on stress/strain distributions in stenotic arteries: 3-D fluid-structure interactions (FSI) models. *J Biomech Eng*. 2004; 126:363–370. [PubMed: 15341174]
72. Tecelao SR, Zwanenburg JJ, Kuijter JP, Marcus JT. Extended harmonic phase tracking of myocardial motion: improved coverage of myocardium and its effect on strain results. *J Magn Reson Imaging*. 2006; 23:682–690. [PubMed: 16570245]
73. Tedgui A, Mallat Z. Cytokines in atherosclerosis: pathogenic and regulatory pathways. *Physiol Rev*. 2006; 86:515–581. [PubMed: 16601268]
74. van Soest G, Mastik F, de Jong N, van der Steen AF. Robust intravascular optical coherence elastography by line correlations. *Phys Med Biol*. 2007; 52:2445–2458. [PubMed: 17440245]
75. Varnava AM, Mills PG, Davies MJ. Relationship between coronary artery remodeling and plaque vulnerability. *Circulation*. 2002; 105:939–943. [PubMed: 11864922]
76. Vengrenyuk Y, Carlier S, Xanthos S, Cardoso L, Ganatos P, Virmani R, Einav S, Gilchrist L, Weinbaum S. A hypothesis for vulnerable plaque rupture due to stress-induced debonding around cellular microcalcifications in thin fibrous caps. *Proc Natl Acad Sci USA*. 2006; 103:14678–14683. [PubMed: 17003118]
77. Virmani R, Burke AP, Farb A, Kolodgie FD. Pathology of the vulnerable plaque. *J Am Coll Cardiol*. 2006; 47:C13–C18. [PubMed: 16631505]
78. Virmani R, Kolodgie FD, Burke AP, Farb A, Schwartz SM. Lessons from sudden coronary death: a comprehensive morphological classification scheme for atherosclerotic lesions. *Arterioscler Thromb Vasc Biol*. 2000; 20:1262–1275. [PubMed: 10807742]
79. Wan M, Li Y, Li J, Cui Y, Zhou X. Strain imaging and elasticity reconstruction of arteries based on intravascular ultrasound video images. *IEEE Trans Biomed Eng*. 2001; 48:116–120. [PubMed: 11235583]
80. Wang JC, Normand SL, Mauri L, Kuntz RE. Coronary artery spatial distribution of acute myocardial infarction occlusions. *Circulation*. 2004; 110:278–284. [PubMed: 15249505]
81. Weydahl ES, Moore JE. Dynamic curvature strongly affects wall shear rates in a coronary artery bifurcation model. *J Biomech*. 2001; 34:1189–1196. [PubMed: 11506789]
82. Williamson SD, Lam Y, Younis HF, Huang H, Patel S, Kaazempur-Mofrad MR, Kamm RD. On the sensitivity of wall stresses in diseased arteries to variable material properties. *J Biomech Eng*. 2003; 125:147–155. [PubMed: 12661209]
83. Zeng D, Ding Z, Friedman MH, Ethier CR. Effects of cardiac motion on right coronary artery hemodynamics. *Ann Biomed Eng*. 2003; 31:420–429. [PubMed: 12723683]



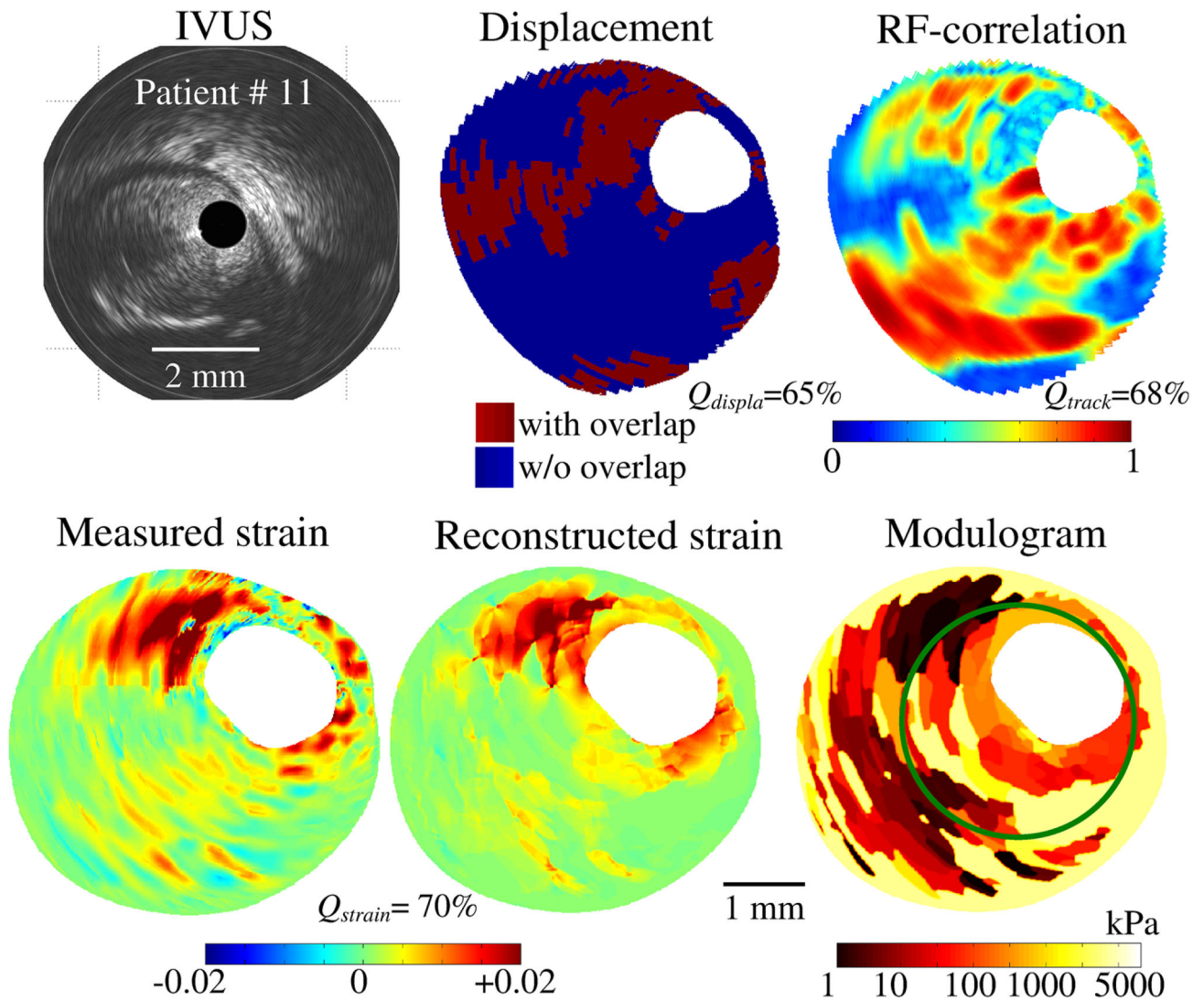
**FIGURE 1.**

Correlation between luminal wall stiffness and localization of atherosclerotic lesions. (a) The statistical analysis was performed by considering several arterial wall regions likely to experience low WSS. (b) Our results highlighted that even within low WSS regions there is an additional and significant correlation between the mean luminal wall stiffness and plaque sites at LAD and LCx. LM: left main coronary artery, LAD: left anterior descending artery, LCx: left circumflex artery. Adapted from Fig. 7 of Ohayon *et al.*<sup>62</sup>





**FIGURE 2.** Three-dimensional plot highlighting the influences of remodeling index and relative necrotic core thickness on critical cap thickness. The critical cap thickness is defined as the value at which cap stress reaches the critical or rupture point tensile stress. This result shows that there is no single such threshold. Rather this cap rupture thickness depends strongly on remodeling index and relative necrotic core thickness. More interestingly, plaques with low remodeling index and a large relative necrotic core thickness can be seen to be more prone to rupture, with a high critical cap thickness. This finding may explain, on the one hand, the progression and growth of clinically silent lesions and, on the other, why plaques with relatively small stenoses have been observed to frequently rupture. Adapted from Fig. 5 of Ohayon *et al.*<sup>60</sup>

**FIGURE 3.**

Performance of the iMOD reconstruction technique<sup>47</sup> and the four-criterion selection procedure of Le Floc'h *et al.*<sup>45</sup> to extract plaque morphology and elasticity map from the IVUS sequence of patient # 11. Note that regions with tissue overlap, observed in the displacement map, correlate well with low RF-correlation coefficient sites. The high value of the strain quality index found ( $Q_{strain} = 70\%$ ) indicates that the method reproduced reasonably the measured radial strain field. The green contour in the modulogram corresponds to the boundary of the lesion that was excised during the directional coronary atherectomy (DCA) procedure.

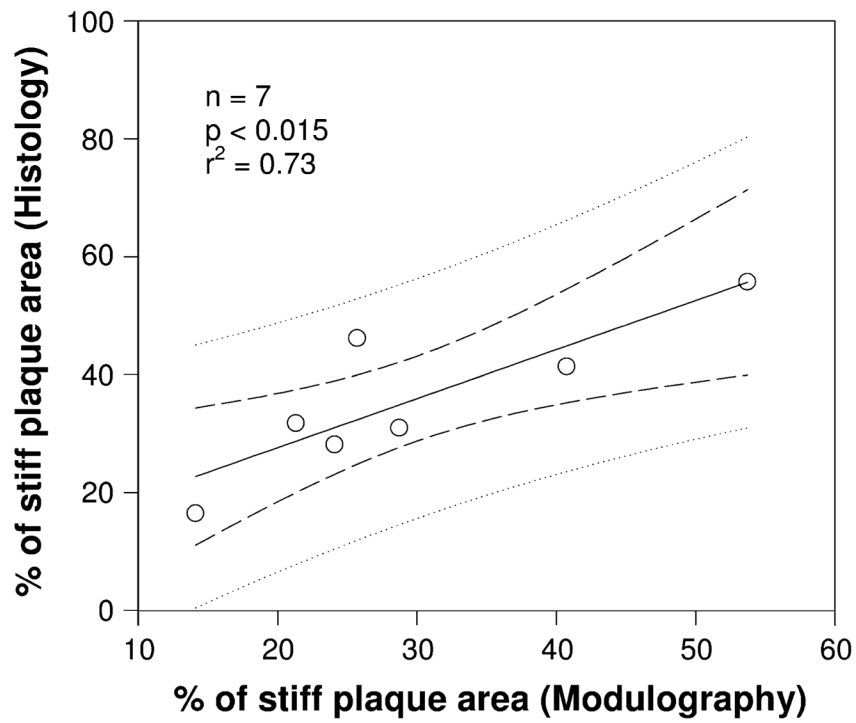


**FIGURE 4.**

A good agreement was found when comparing the percentage of stiff plaque area (i.e., with Young's modulus >700 kPa) values derived from the computed modulograms with the percentage of plaque area with high collagen content obtained from the histological analyses of the excised plaque samples. The linear regression line (dark line) and the confidence of the prediction interval domains, which are the domains limited by the two internal and external dashed lines, respectively, are also given. Adapted from Fig. 8 of Le Floc'h *et al.*<sup>45</sup>

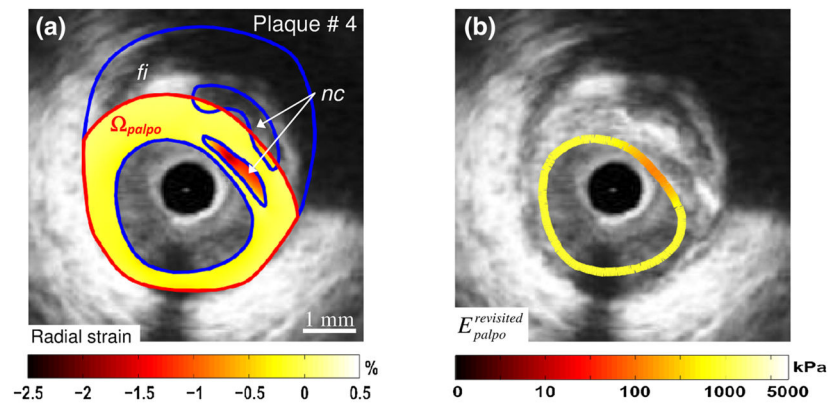


**FIGURE 5.**

Performance of the improved E-PT of Deleaval *et al.*<sup>19</sup> to detect a complex vulnerable plaque with two necrotic cores. (a) IVUS image of plaque # 4 with plaque constituents (blue contours, “nc”: necrotic core; “fi”: fibrous region). The external boundary of the palpography domain  $\Omega_{palpo}$  is given (red contours). The measured radial strain-elongation in the palpography domain  $\Omega_{palpo}$  is also presented. (b) Computed improved S-SM palpogram. The color coded strip superimposed on the IVUS image gives at each circumferential point the computed modulus over the corresponding radial thickness of the plaque. This result illustrates the abilities of the proposed technique to detect the soft inclusions located between 1 and 3 o'clock.